NANO · MICRO small
www.small-journal.com

Selective Ion Sensing in Artificial Sweat Using Low-Cost Reduced Graphene Oxide Liquid-Gated Plastic Transistors

Rafael Furlan de Oliveira, Verónica Montes-García, Pietro Antonio Livio, María Begoña González-García, Pablo Fanjul-Bolado, Stefano Casalini, and Paolo Samorì**

Health monitoring is experiencing a radical shift from clinic-based to point-of-care and wearable technologies, and a variety of nanomaterials and transducers have been employed for this purpose. 2D materials (2DMs) hold enormous potential for novel electronics, yet they struggle to meet the requirements of wearable technologies. Here, aiming to foster the development of 2DM-based wearable technologies, reduced graphene oxide (rGO)-based liquid-gated transistors (LGTs) for cation sensing in artificial sweat endowed with distinguished performance and great potential for scalable manufacturing is reported. Laser micromachining is employed to produce flexible transistor test patterns employing rGO as the electronic transducer. Analyte selectivity is achieved by functionalizing the transistor channel with ion-selective membranes (ISMs) via a simple casting method. Real-time monitoring of K^+ and Na^+ in artificial sweat is carried out employing a gate voltage pulsed stimulus to take advantage of the fast responsivity of rGO. The sensors show excellent selectivity toward the target analyte, low working voltages (<0.5 V), fast (5–15 s), linear response at a wide range of concentrations (10 µM to 100 mM), and sensitivities of 1 µA/decade. The reported strategy is an important step forward toward the development of wearable sensors based on 2DMs for future health monitoring technologies.

1. Introduction

The unique electrical, mechanical, thermal, optical, and electrochemical properties of two-dimensional materials (2DMs) have triggered a major scientific revolution during the past two decades with unparalleled efforts devoted toward their synthesis,[1–3] functionalization,[4] and application in (opto)electronics,[5] energy[6] and sensing.[7] However, from a technological perspective, there are still some issues that must be addressed to exploit the full potential of 2DMs in everyday applications. This involves the production of high-quality and industrially-scalable 2DMs at accessible prices, the development of robust functionalization methods compatible with industrial practices, the use of affordable and scalable manufacturing technologies, and the establishment of efficient protocols to incorporate them into marketable technologies.[4]

Among the plethora of available 2DMs, graphene oxide (GO) represents a versatile and suitable material whose processability complies with industrial fabrication requirements (e.g., large-scale solution production) and the abundance of oxygen groups (namely hydroxyl, carboxyl, epoxide, etc.) is ideal for its post-processing functionalization.[8,9] Although GO is not electrically conductive, its reduced form (rGO) exhibits elevate conductivities (>1000 S cm^{-1}) that are well-suited for different electronic applications such as resistors, supercapacitors, sensors, biosensors, etc.[8,10,11] So far, various types of methods have been reported to obtain conductive rGO sheets[10,12,13] by making use of chemical,[14] photochemical,[15] thermal,[16] photothermal,[17] ultrasound or microwave-assisted,[18] and electrochemical reduction processes.[19–21] In particular, the latter has been extensively used mainly for standard electrochemical applications[22] where rGO films are employed as carbonaceous electrodes produced with simple laboratory apparatus. The GO electrochemical reduction holds enormous potential for plastic and flexible electronics featuring a whole green device manufacturing process since it can be carried out in the absence of toxic reductant agents, at high throughput, and low processing costs, especially when combined with rapid device prototyping technologies.[19]

Marketable technologies for wearable chemical sensing must inevitably combine a set of unique characteristics that

R. Furlan de Oliveira, V. Montes-García, P. A. Livio, S. Casalini, P. Samorì
Université de Strasbourg
CNRS
ISIS UMR 7006, 8 allée Gaspard Monge, Strasbourg F-67000, France
E-mail: stefano.casalini@unipd.it; samori@unistra.fr
R. Furlan de Oliveira
Brazilian Nanotechnology National Laboratory (LNNano)
CNPEM
Campinas 13083–970, Brazil
M. B. González-García, P. Fanjul-Bolado
Metrohm DropSens,S.L.
Vivero de Ciencias de la Salud
C/ Colegio Santo Domingo de Guzmán s/n
Oviedo, Asturias 33010, Spain
S. Casalini
Università degli Studi di Padova
Dipartimento di Scienze Chimiche
via Marzolo 1, Padova 35131, Italy
The ORCID identification number(s) for the author(s) of this article can be found under https://doi.org/10.1002/smll.202201861.

DOI: 10.1002/smll.202201861

are beyond traditional laboratory analytical tools.[23,24] These encompass not only the engineering aspects of the envisioned wearable, for example, the device manufacturing processes, but also those of applied chemistry and materials functionalization responsible for the analyte recognition in complex media (namely sweat) and signal transduction.[23,24] Thus, neither an intricate or indiscriminate combination of materials to attain analyte detection nor handcrafting device fabrication can serve as feasible routes for the development of marketable wearable chemical sensors. Instead, a synergy must exist between the most suitable device manufacturing processes and the sensor analytical performance.

From the manufacturing perspective, laser micromachining is recognized as a versatile tool for rapid fabrication of flexible electrodes and test patterns with no need of using photolithography, wet chemical methods (e.g., lift-off and etching), and a cleanroom environment.[11,25,26] Although photolithography is still a benchmark for device manufacturing, laser micromachining of metal and dielectric films allows the prompt patterning of microstructures featuring different shapes and arrangements on nearly any surface, at high throughput, and is compatible with an on-demand changeability of device layouts.[25,27] Another advantage of laser micromachining is its well-suited compatibility with an industrial production line containing a variety of other techniques for the manufacturing of plastic electronics, such as roll-to-roll.[28]

From the analytical sensing viewpoint, ion-selective membranes (ISMs) have been extensively employed for the selective determination of ions,[29,30] with the pH-meter representing the most successful ISM-based sensor technology. ISMs rely on the specific features of ion exchangers such as valinomycin, one of the most used potassium (K^+) ionophores, capable to confer ion-specificity to the membrane.[31,32] Ion-sensitive field-effect transistors (ISFETs) can directly integrate an ISM onto a semiconducting material, thereby minimizing the precious amount of ionophore employed for the fabrication of an ion-selective electrode due to its straightforward device miniaturization.[32,33] Although graphene-based ISFETs have already shown an excellent performance as cation sensors,[31] most devices are typically produced with lab-scale methods, thus lacking compatibility with the stringent requirements for wearable chemical sensing technologies.[24,34] rGO-based transistors are highly advantageous for wearable electronics, both from the device manufacturing perspective and the rGO physicochemical properties. rGO films can be produced from aqueous GO dispersions (i.e., no toxic organic solvents involved) onto plastic and biocompatible substrates,[19] which are essential for wearable applications. Additionally, rGO has been reported to be non-irritating for the skin,[35,36] where a lesser degree of oxidation implicates in lower cytotoxicity to epidermal cells (keratinocytes).[36] The rGO conductivity (and therefore its degree of oxidation) can be controlled via a variety of reduction methods (e.g., electrochemical, thermal, chemical, etc.), which makes it a material with adjustable properties.[10] Finally, rGO transistors are also ambipolar without requiring any contact engineering.[19,37] This means that both positive (holes) and negative (electrons) charge carriers are responsible for the device current response, giving one more output signal or quantifiable parameter during sensing of cationic and anionic species. These altogether characteristics cannot be found in other 2DM-based transistors for wearable sensing technologies.

Here we report on the production of an ion-selective plastic rGO liquid-gated transistors (LGTs) for the detection of K^+ and Na^+ in artificial sweat which combines all features needed in chemical sensors to be readily upgraded to wearable technologies. The device manufacturing was devised to be consonant with the industrial scalable process, as it comprises: i) the laser-ablation patterning of flexible Au electrodes; ii) the straightforward casting of a GO aqueous dispersion and its green electrochemical reduction (water is the unique solvent used); iii) the rGO functionalization with ion-sensitive membranes (ISMs) on the transistor channel; and iv) handling of paper-based fluidics for dosing spiked analyte solutions to the LGT sensor. The sensor has been challenged by using artificial sweat as a complex matrix by taking full advantage of the intrinsic high signal amplification ability of LGTs and their operation at low voltages (<0.5 V). Two sensing tests have been successfully demonstrated: the former relies on standard voltage sweep measurements, namely current–voltage (I–V) transfer characteristics, and the latter on gate voltage pulse and time-dependent current recording. Gate voltage pulsed measurements are preferable to avoid typical signal drifting observed during real-time analyte monitoring[38] and common hysteresis during the transistor operation under voltage sweep.[39] The rGO-based LGT sensor displayed excellent selectivity toward the target analyte, namely, no interference of Na^+ cations during K^+ determination in artificial sweat, along with a linear sensitivity of S = 1.169 (±0.091) and 1.04 (±0.03) μA/pK^+ for the respective current recording methods (i.e., gate voltage sweeping and pulsing), within a large [K^+] range (from 10 μM to 100 mM). By employing the gate voltage pulse approach, the K^+ concentration could be determined as fast as 5 s after the beginning of the current recording. Na^+ sensing in artificial sweat was realized by employing a Na^+-ISM on the rGO LGT channel. Such a prompt determination of the target analyte is highly advantageous for applications in wearable electronics where continuous cation monitoring is necessary, for example, for sweat analysis during a workout as a rich source of physiological information for health monitoring.

2. Experimental Section

2.1. Materials

Here the authors used polyethylene terephthalate (PET) substrates (175 μm thick) from Metrohm DropSens, poly(diallylmethylammonium chloride solution (PDDA) from Sigma Aldrich, graphene oxide (GO) - 4 mg mL^{-1}, monolayer content >95%, lateral flake size <10 μm - from Graphenea, CN 140 nitrocellulose paper (130 μm thick) from Unisart. Artificial sweat ISO-3160-2 (from Reagents) containing 20 g L^{-1} NaCl (or KCl, depending on the employed artificial sweat formulation), 17.5 g L^{-1} NH_4Cl, 1.5 g L^{-1} lactic acid, 5 g L^{-1} urea and 2.5 g L^{-1} acetic acid, with pH adjusted to 4.7 with NaOH. Selectophore grade potassium ionophore I (valinomycin) and sodium ionophore X, potassium tetrakis(4-chlorophenyl) borate (≥98.0%), bis(2-ethylhexyl) sebacate (≥97.0%), poly(vinyl

chloride) (PVC), and tetrahydrofuran (THF) were purchased from Sigma-Aldrich and used without any further purification steps.

2.2. Fabrication of Plastic rGO LGTs

Transistor test patterns were fabricated on Au-coated PET by laser ablation. PET foils sputter-coated with 20 nm Au layer were ablated by Nd:YAG laser (532 and 1064 nm wavelengths, tunable power) in an automated laser scribing station (Rofin, Germany) to produce a pair of interdigitated metallic electrodes (IDEs) and a coplanar gate electrode. IDEs were produced with 12 digits, with channel length (L) equal to 30 µm and width (W) of 690 µm. The coplanar gate electrode possesses a 9 mm^2 area, positioned 4 mm distant from the IDEs. The authors also produced contact pads compatible with 6-pin zero insertion force (ZIF) connectors commonly used in printed circuit boards for portable and wearable electronics.[40,41] The PET test pattern configuration is depicted in **Figure 1**. Additional details can be found in the Supporting Information.

To fabricate rGO LGTs, PET test patterns were cleaned with isopropanol, water, and blown dry in N_2. A drop (5 µL) of PDDA aqueous solution (1% w/w) containing 0.5 mol L^{-1} of NaCl was placed onto the IDE region for 15 min to allow the polyelectrolyte deposition on the surface and rinsed thoroughly in water thereafter. GO suspension (0.4 mg mL^{-1}) was sonicated for 1 min for improved homogeneity before deposition. A drop of GO solution was placed on the PDDA-functionalized surface for 30 min, rinsed abundantly with water, and dried under a gentle N_2 flow. To prevent the solvent evaporation during assembly

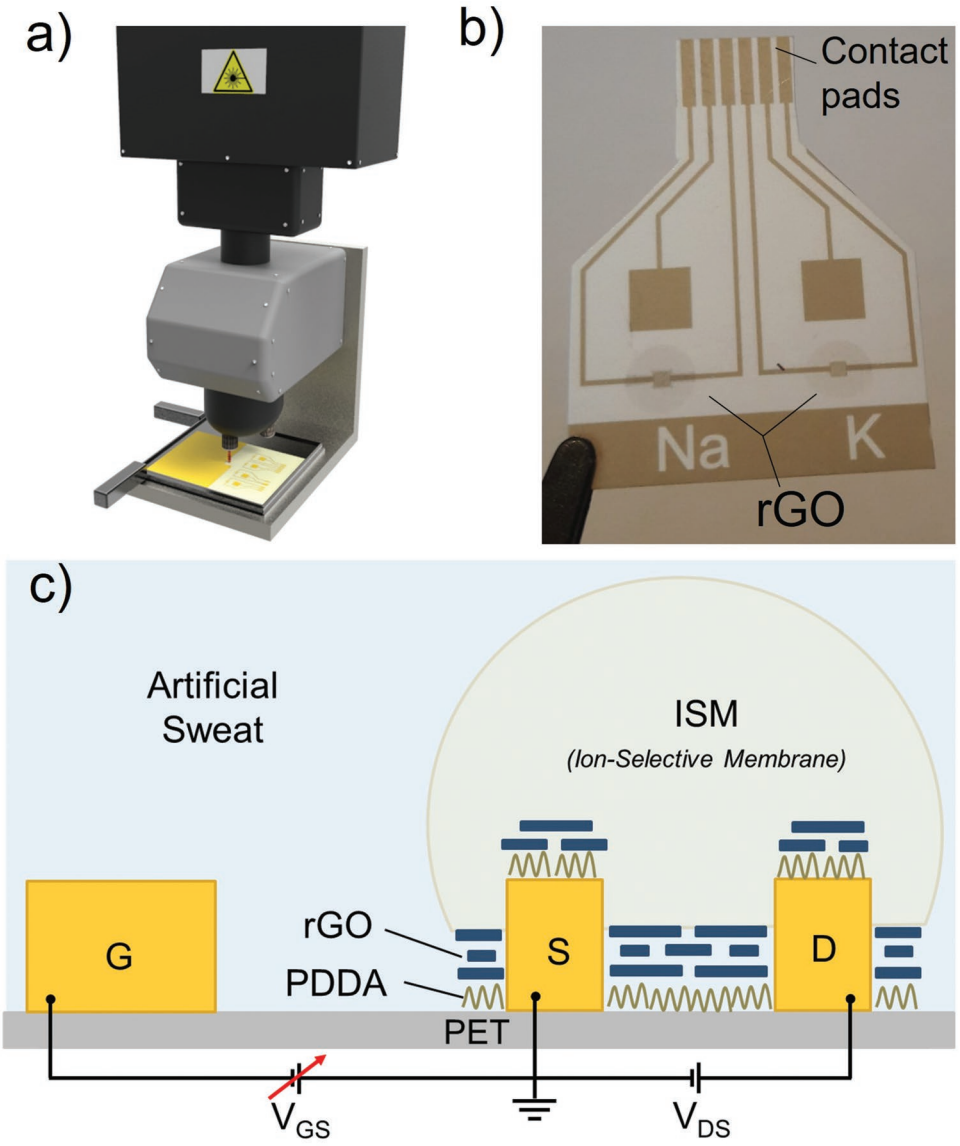

Figure 1. a) Laser micromachining setup for the ablation of Au-coated plastic foils and the production of LGT test patterns. b) Photograph of plastic rGO LGTs. The device dimension is 1.5 cm wide and 2.5 cm long. c) Schematic representation of the rGO LGT cross-section employing an ion-selective membrane (ISM). Gate (G), source (S) and drain (D) terminals and the electrical connections are indicated.

and inhomogeneous film formation, the PDDA and GO depositions were carried out inside a sealed glassware by establishing a saturated humidity environment through the placement of a small water reservoir (this allows a patterned cast of the material of interest for an arbitrary time, namely from minutes to days free of any uncontrolled effects due to convective material motion). Finally, GO was electrochemically reduced by cyclic voltammetry in water. For this purpose, the GO-coated IDEs were short-circuited to act as the working electrode (WE) in the electrochemical setup using a Metrohm Autolab PGSTAT 204 potentiostat/galvanostat. A droplet of bi-distilled water (≈50 µL) is positioned onto the GO-coated region with an external polycrystalline Au plate (area ≈0.031 cm^2) sitting atop the counter (CE)/reference (RE) single electrode. Few (1–4) voltammetric cycles, sweeping WE potential from 0 to −2.8 V at a scan rate of 100 mV s^{-1}, are sufficient to achieve the reduction of the GO thin-film. Further details on the green GO electrochemical reduction employed here to fabricate plastic rGO LGTs can be found elsewhere.[19]

2.3. Preparation of ISMs and Artificial Sweat

K^+ and Na^+ selective membranes were prepared from their respective stock solutions containing the individual ionophores (2 wt%), tetrakis(4-chlorophenyl)borate (0.5 wt%), bis(2-ethylhexyl) sebacate (64.7 wt%) and PVC (32.8 wt%) in THF, featuring a final concentration of 20 mg mL^{-1}. Freshly prepared cocktails were diluted in THF in a 1:5 ratio and stored in the fridge (3 °C). Stock solutions and formulations were stored for no longer than 2 weeks. ISM formulations were drop-casted (<5 µL) onto rGO at the device IDE region and left to dry at room temperature. Before the measurements, the respective ISM-coated devices were conditioned in 1 mM KCl or 1 mM NaCl for 30 min, depending on the chosen ISM coating. The surface characteristics and thickness of the ISM coating onto the rGO LGT channel were determined by scanning electron microscopy (Quanta FEG 450) and profilometry (KLA-Tencor Alpha-Step IQ). Additional morphological characterization of the device was accomplished by means of laser scanning confocal microscopy (Keyence VK-X200) and atomic force microscopy (Park Systems – NX10).

Two formulations of artificial sweat, with different Na^+- and K^+-free compositions, were prepared. Then, Na^+ (or K^+) was controllably introduced in the respective cation-free artificial sweat composition at the desired concentration by using NaCl (or KCl). Artificial sweat formulations having controlled Na^+ (or K^+) with concentrations ranging from 10 µM to 100 mM, which is representative in real human sweat and related pathologies whose diagnostics can be achieved via sweat analysis, were prepared.[41–43]

2.4. Electrical Measurements

The *I–V* transfer characteristics of rGO LGTs were probed in solution by measuring their source-drain current (I_{DS}) while sweeping the gate-source (V_{GS}) from −0.4 to +0.4 V, at a rate of 20 mV s^{-1}, and at a constant source-drain (V_{DS}) voltage of 100 mV. The transistor source-gate leakage current (I_{GS}) as a function of V_{GS} was also measured to verify the proper device operation. For each *I–V* transfer measurement in each condition, three curves were recorded for the sake of the device stability. Additionally, time-dependent current measurements under pulsed gate voltage were performed at constant V_{DS} (100 mV) and under V_{GS} pulse from 0 to −400 mV. Both measurements were performed in spiked artificial sweat solutions containing the target cationic specie (K^+ or Na^+). The artificial sweat solution was confined on the transistor surface with the assist of a nitrocellulose paper membrane suitably positioned over the gate and channel regions.[19] All electrical measurements were carried out using a probe station, in ambient conditions, connected to a Keithley 2636A SourceMeter unit.

3. Results and Discussion

Aiming to develop highly sensitive and selective ion sensors employing a manufacturing strategy compliant with the stringent requirements of wearable electronics, the first relevant fabrication step we employed resides in the extensive use of laser ablation to produce low-cost, plastic transistor test patterns (Figure 1a). As prototypical architecture, we focused on a device layout comprising source and drain IDEs and a coplanar gate electrode, as portrayed in Figure 1b. This blueprint enables a compact and self-standing platform that can be easily connected to external portable circuitry via a ZIF connector (Supporting Information).[19] Although the laser ablation of plastic test patterns is a rapid prototyping method, it unavoidably leads to the roughening of the target substrate, which here was found to exhibit a root mean square roughness of ca. 60 nm.[19] High surface roughness can jeopardize the performance of thin-film devices (including LGTs), especially those based on organic semiconductors where molecular packing at the substrate surface plays a major role in the long-range electronic conduction.[44,45] Here, because long-range electronic conduction in rGO thin films possesses a significant intraflake transport contribution,[46] such a deleterious effect derived from elevated roughness of laser-patterned substrates does not compromise the device operation. Another surface-related issue is the poor adhesion of GO onto PET, which required the use of a strong polyelectrolyte (PDDA) as an adhesive layer to guarantee a homogenous and robust coating capable to withstand the electrical stress during the GO electrochemical reduction and the following transistor operation.[19] Details on the rGO film morphology, uniformity and flake size can be found in Figures S1–S3, Supporting Information.

To ensure a full reproducibility of our fabrication protocol, we systematically monitored: i) the electrical resistance of the laser-ablated Au electrode tracks on plastic; and ii) the rGO transistor channel resistance. For the sake of reproducibility, we measured electrodes produced from several different batches (Figure S4, Supporting Information). The laser-ablated Au-coated PET foil produced electrode tracks with low (<600 Ω) and uniform resistances (statistics taken for ca. 40 devices), which are sufficiently low to allow LGT operation. Regarding the rGO films in the transistor channel, the Au/rGO is ohmic and the typical rGO resistance is 2–15 kΩ (Figure S5, Supporting Information). Additionally, to validate our manufacturing protocol, we characterized

the rGO LGT operation in water, as shown in Figure S6, Supporting Information. Finally, the casting of the ISM (K^+-ISM) onto the channel surface produces only minor resistance variations (ΔR), which implies that the functional coating does not affect the rGO electronic properties (Figure S7, Supporting Information). We can infer that our whole fabrication protocol fulfils the morphological, robustness, and electronic demands for a flexible transistor sensing device. The Figure 1c illustrates the device cross-section containing the ISM, the rGO film, the LGT Au electrodes and respective electrical connections.

Before the sensing experiments in artificial sweat, we validated the rGO LGTs operation and characteristics in Milli-Q water (Figures S6, Supporting Information), where we found the charge carrier mobility (μ) of holes and electrons in the rGO film corresponding to μ_h = 0.026 (±0.014) $cm^2\ V^{-1}\ s^{-1}$ and μ_e = 0.17 (±0.015) $cm^2\ V^{-1}\ s^{-1}$, respectively. These values agree with those typically reported for LGTs employing electrochemically produced rGO.[19] After that, we investigated the sensing properties of the pristine (ISM-free) rGO-based LGTs operating in artificial sweat (**Figure 2**). The *I–V* transfer characteristics do not show any significant electrical noise or instability due to the device operation in artificial sweat, which contains hundreds of millimolars' concentration of ionic species (K^+, Na^+, Cl^-, NH_4^+). Furthermore, the device shows the typical ambipolar behavior of graphene transistors, characterized by a broad Dirac point (V_{Dirac})—namely V_{GS} when I_{DS} reaches its minimum value—close to −50 mV.[19,47] No electrical failures have been recorded if positive V_{GS} values higher than 500 mV are avoided. Instabilities and failures under elevated electrical potentials are typically ascribed to the etching of Au electrodes and contact leads for devices operating in highly-concentrated electrolytes, a process assisted by the presence of a high concentration of chloride anions.[48] Regarding the ion sensing response, the increasing concentration of K^+ in artificial sweat does not lead to significant changes in the *I–V* transfer characteristics of pristine rGO devices (Figure 2a). Upon the increase of K^+ concentration, no clear sensitivity toward this cation has been observed for any V_{GS} applied (0 V < V_{GS} < −0.4 V). A poor correlation between I_{DS} and the K^+ concentration (pK^+) was found, indicated by a coefficient of determination (R^2)—from the linear fit of data in Figure 2b—that attains only 0.554 for V_{GS} = −0.4 V when the signal is higher. The device sensitivity (S) and R^2 for pristine rGO LGTs at different applied V_{GS} in the presence of K^+ are given in Table S1, Supporting Information. Similarly, no specificity has also been observed for Na^+ ions either (Figure S8 and Table S2, Supporting Information). For both species, no variations in the transistor leakage current (I_{GS} versus V_{GS}) that could be associated with the presence or concentration of the respective cations were observed (Figure S9, Supporting Information). Such a lack of selectivity and sufficient sensitivity hamper the fabrication of an efficient ion sensor to be operated in complex matrixes, such as sweat if no rGO functionalization is employed. Finally, other graphene-related transistor sensors in the literature exploit the V_{Dirac} shift as the main indicator for the detection of various analytes, including ionic species[29,49] Here, pristine (ISM-free) devices exhibit a broad V_{Dirac} around −50 mV, characteristic of defective rGO films,[19,50] whose position is not effectively altered regardless of the different cation concentrations (Figure 2a).

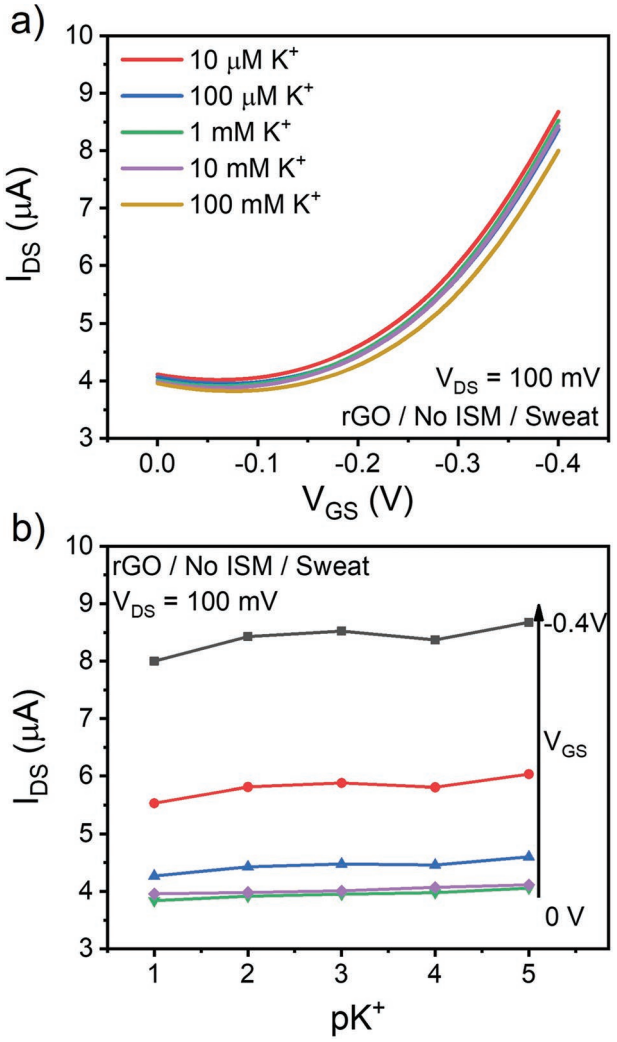

Figure 2. a) *I–V* transfer characteristics of pristine (ISM-free) rGO LGT in artificial sweat (V_{DS} = 100 mV) at different K^+ concentrations. b) Corresponding I_{DS} as a function of K^+ concentration (log-scale) at different constant V_{GS}.

To simultaneously confer improved cation sensitivity and selectivity to the rGO LGTs, the integration of an ISM is necessary. As previously discussed, the casting of an ISM onto the rGO surface does not significantly affect its electrical properties (Figure S7, Supporting Information). Concerning the operation of the ISM-functionalized transistor, conditioning steps are necessary to ensure proper ion sensing ability. First, devices having an as-prepared ISM coating are exposed to a 1 mM saline solution of the cation of interest (KCl or NaCl) for 30 min, a routine step for ISM-based technologies.[51] Second, for measurements carried out in artificial sweat, a 5 s exposure time was employed to minimize the influence of membrane polarization effects. These steps do not affect the transistor operation, namely the V_{GS} window or scan rate employed, as the thickness of the ISM membrane is considered reasonably thin (≈2 μm) to not compromise the formation of the electric double layer at the device interface (Figures S10 and S11, Supporting Information).

Figure 3a exhibits the transfer characteristics of ISM-functionalized rGO LGTs for different K^+ spiked solutions

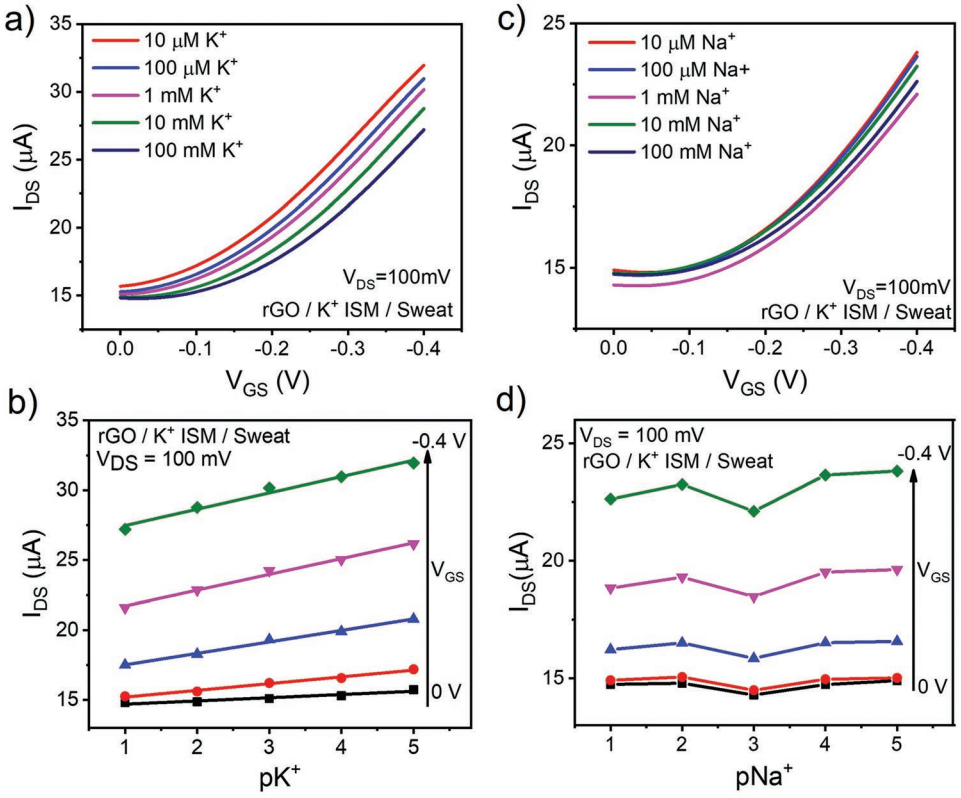

Figure 3. a) K^+-ISM functionalized rGO LGT transfer characteristics recorded in K^+-spiked solutions of artificial sweat; b) sensitivity plots: I_{DS} versus K^+ concentration (log-scale). c) K^+-ISM functionalized rGO LGT transfer characteristics recorded in Na^+-spiked solutions of artificial sweat; d) sensitivity plots: I_{DS} versus Na^+ concentration (log-scale).

of artificial sweat (namely from 10 μM to 100 mM). One can observe a clear negative shift of the I_{DS} values (i.e., toward more negative V_{GS}) as the K^+ concentration increases. Such a response can be ascribed to the built-in potential at the interface between the artificial sweat and the K^+-ISM, which conveys the gradient of cations inside and outside the K^+-ISM. This yields a decrease in the number of hole carriers flowing within the rGO transistor channel for the applied V_{GS} range. The sensitivity plot (Figure 3b)—namely the I_{DS} versus [K^+] plot—shows a linear trend for K^+ concentrations between 100 mM and 10 μM (log-scale). Concerning the effect of the gate bias, the highest V_{GS} shows the highest sensitivity, namely $S = 1.169$ (±0.091) μA/pK^+ with an excellent correlation featuring R^2 equal to 0.976. The S values extracted for other applied V_{GS} biases are reported in Table S3, Supporting Information. Although the use of complex media such as artificial sweat guarantees a deep study of the sensor sensitivity and selectivity, the latter has been further evaluated by using Na^+ spiked artificial sweat solutions for devices containing a K^+-ISM coating. Na^+ is one of the most challenging interfering cations while using K^+-ISM due to the physical-chemical similarities between the two ionic species, namely they are both monovalent spherical alkali cations with similar ionic radii (1.02 and 1.38 Å for hexacoordinated Na^+ and K^+, respectively[52,53]). From Figure 3c,d, the device selectivity has been validated as no clear I_{DS} correlation with the increase of Na^+ concentration was observed (no linear correspondence between I_{DS} and [Na^+] with $R^2 > 0.17$ could be obtained). Finally, no effect on the device leakage current (I_{GS}) as a function of the cation concentration (either for K^+ or Na^+) was observed, indicating that the I_{DS} variations arise from the functionalized ISM coating that confers to the rGO transistors' high selectivity and sensitivity (Figure S12, Supporting Information).

Despite the achieved sensitivity and selectivity verified from the transfer characteristics of ISM-functionalized rGO LGTs, such an operation mode (i.e., V_{GS} sweeping) is not the most suited aiming a real-time monitoring of K^+ cations. This is because sensing based on voltage sweeping can be rather slow, or even produce hysteresis or irreproducible response if dwell time is not sufficient (Figure S13, Supporting Information). By targeting a more straightforward ion detection method, we performed the real-time monitoring of K^+ under constant V_{GS} and V_{DS} biases. For this purpose, a wax-patterned paper membrane has been tailored onto the device to act as a low-cost fluidic system by taking advantage of the appropriate paper capillarity to handle small amounts of liquids (a few microliters), as shown in Figure S14a, Supporting Information. The response of self-standing rGO LGTs has been monitored continuously during different [K^+] variations (Figure S14b, Supporting Information). Even though the K^+ monitoring succeeded, current drifting makes this type of test inconvenient for direct monitoring of the target species. This type of response may thus require post-measurement signal treatments (e.g., baseline correction), thereby risking losing information on the sensor sensitivity. Consequently, current monitoring at a fixed voltage bias for

long durations does not seem suitable for real-time cation sensing using this kind of approach. To circumvent this, we adopted pulsed voltage measurements, namely a combination of a single step V_{GS} pulse at constant V_{DS} while monitoring I_{DS} for short time intervals, namely shorter than 30 s (**Figure 4**a). This method minimizes the current drifts issues.[38]

Figure 4b shows the time-dependent response of the K^+-ISM functionalized rGO LGTs at different concentrations of K^+ in artificial sweat. The transistor channel current (I_{DS}) was monitored for a short time (30 s) upon a V_{GS} pulsed stimulus of –400 mV within the same interval, with V_{DS} fixed at 100 mV. We chose V_{GS} = –0.4 V because it produces the larger current signals. We observed that upon the V_{GS} voltage pulse, I_{DS} rapidly increases and reach a steady-state current level for the different K^+ concentration because of the formation of the electrical double layers at the device's interfaces. Although the device I_{DS} exhibits slow decay over time for some measurements, such a time interval (30 s) is sufficient to establish a correlation between the registered current and the respective K^+ concentration. Figure 4c displays the device sensitivity plot (I_{DS} versus K^+ concentration) from the pulsed measurements. Three acquisition times have been systematically compared, namely 5, 15 and 30 s, and the shortest one has shown the best sensitivity S = 1.04 (±0.03) μA/pK^+. The calculated S values for other acquisition times are given in Table S4, Supporting Information. The implemented approach was also deployed for Na^+ sensing by employing rGO LGTs functionalized with a Na^+-ISM (Figure S15 and Table S5, Supporting Information). The reported method for cation detection not only mitigates the current drift issues but also minimizes the electrical stress on the device, thereby increasing the number of sequential sensing tests that can be performed with a single transistor. Additionally, for wearable sensing technologies, a device that operates just for a short period to register the signal of interest, rather than being continuously biased, seems more practical and energetically viable for real applications.

Diverse chemical sensors aiming at the development of wearable technologies for health monitoring have been reported in the literature.[23,41,54,55] Regarding the detection of cationic species (especially K^+ and Na^+) the use of ISM technology is ubiquitous, and it has been employed to functionalize a plethora of nanomaterials (including 2DMs) and transducers.[23,41,54] To meet the requirements for wearable electronics though, we believe that potential devices must present a unique combination of characteristics, namely operation and response in sweat, distinguished sensing performance and scalable manufacturing technology. **Table 1** summarizes some of the most recent 2DM-based devices for cation sensing and their key performance indicators. Transistor-based cation sensors employing 2DMs are mostly graphene ISFETs.[29,31,32] To the best of our knowledge, all reported 2DM-based transistors employed as cation sensors to date are likely not appropriate for wearable technologies despite presenting outstanding performance indicators, namely elevate sensitivities, selectivity, operation within a broad range of analyte concentration, low detection limits and real-time responsivity. The main limitations of such transistors refer to their non-demonstrated operation in complex media (e.g., sweat or artificial sweat) and/or fabrication incompatible with large-scale manufacturing, for example, by the use of

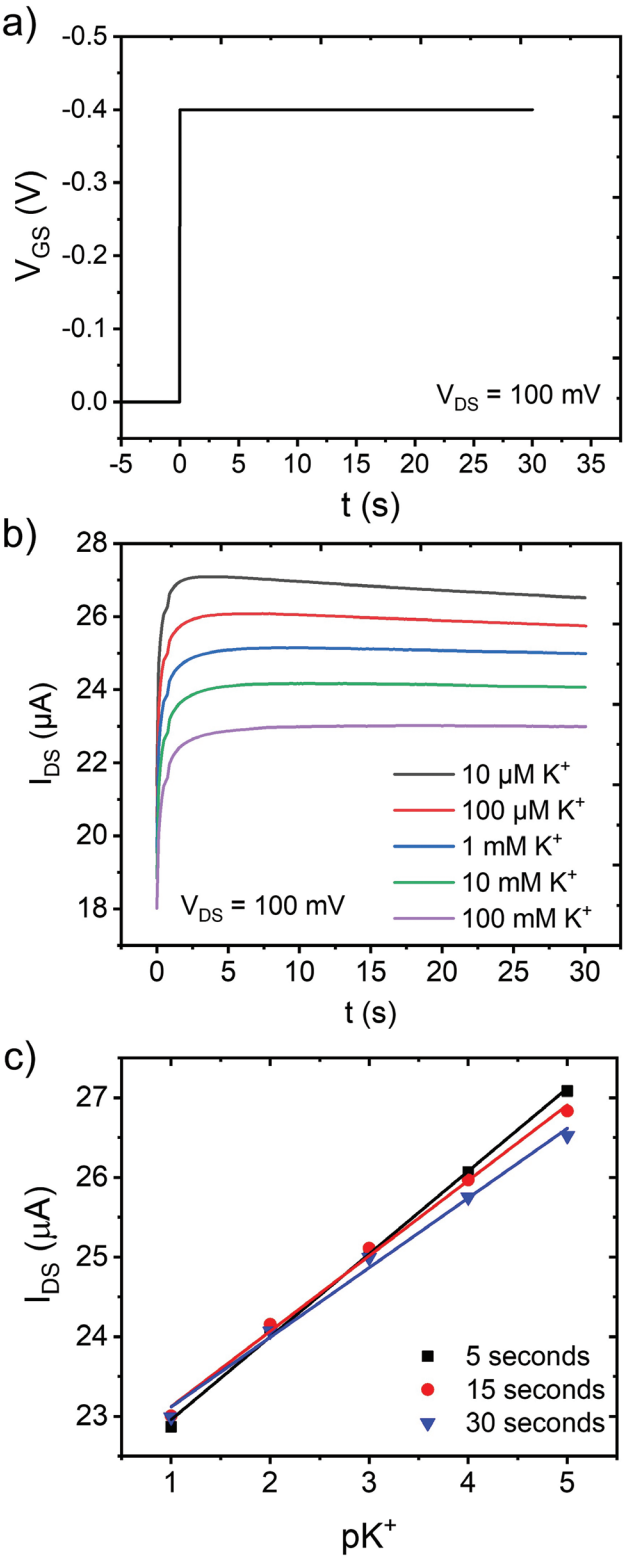

Figure 4. Rapid K^+ sensing employing a K^+-ISM functionalized rGO LGT operating under V_{GS} pulse. a) V_{GS} single pulse as a function of time, at fixed V_{DS} = 100 mV. b) Respective I_{DS} versus time plot for K^+-spiked solutions of artificial sweat at different concentrations. c) Sensitivity plots: I_{DS} versus pK^+ at different acquisition times (5, 15, and 30 s).

Table 1. 2DM-based devices employing ISMs for selective cation sensing and their respective performance indicators.

Active material/ substrate	Device technology	Potential scalable manufacturing	Target cation	Operation in sweat or artificial sweat	Working range	Sensitivity (amperometric or potentiometric)	Selectivity test	Real-time operation/response time	Ref.
CVD graphene/ SiO_2	ISFET	No	K^+, Na^+, NH_4^+	No	10^{-2} to 10^{-6} M (K^+), 10^{-2} to 10^{-5} (Na^+, NH_4^+)	16.92 μA/dec (K^+) 17.43 μA/dec (Na^+) 18.44 μA/dec (NH_4^+)	Yes	Yes, ≈30 s	[29]
CVD graphene/ SiO_2	ISFET	No	K^+	No	10^{-2} to 10^{-9} M	6.58 μA/dec (or 37 mV/dec)	Yes	Yes, <100 s	[31]
CVD graphene/ PET	ISFET	No	K^+	No	10^{-1} to 10^{-6} M	60 mV/dec (potentiometric only)	Yes	Yes, ≈7 s	[32]
Graphene ink/paper	Potentiometric electrode	Yes	K^+, Na^+	Yes	10^{-1} to 10^{-6} M (K^+, Na^+)	57 mV/dec (K^+)* 55.7 mV/dec (Na^+)*	No	Yes, not determined	[56]
LIG on PDMS/lignin	Potentiometric electrode	Yes	K^+, Na^+	Yes	10^{-1} to 10^{-8} M (K^+) 10^{-1} to 10^{-7} M (Na^+)	59.2 mV/dec (K^+)* 63.6 mV/dec (Na^+)*	Yes	Yes, ≈200 s	[57]
rGO/PET	Potentiometric electrode	Yes	K^+, Na^+	Yes	10^{-2} to 10^{-3} M (K^+) 10^{-1} to 10^{-2} M (Na^+)	51.1 mV/dec (K^+)* 42.5 mV/dec (Na^+)*	Yes	Yes, 200 s	[58]
ME-graphene/ SiO_2	LGT	No	K^+	No	10^{-3} to 10^{-8} M	7.8 mV/dec (potentiometric only)	Yes	No	[33]
rGO/PET	LGT	Yes	K^+, Na^+	Yes	10^{-1} to 10^{-5} M (K^+, Na^+)	1 μA/dec (K^+, Na^+)	Yes	Yes, 5–15 s	This work

Abbreviations: CVD - chemical vapor deposition, ME - mechanical exfoliation, rGO - reduced graphene oxide, PET - polyethylene terephthalate, ISM - ion-selective membrane, ISFET - ion-sensitive field-effect transistor, LGT - liquid-gated transistor, LIG - laser-induced graphene, PDMS - polydimethylsiloxane. *Values determined in aqueous electrolyte before sensing in sweat.

graphene obtained from mechanical exfoliation (ME), chemical vapor deposition (CVD), and/or by employing rigid substrates. Currently, the most promising 2DM-based cation sensors for wearable applications that present concomitant: i) potential scalable manufacturing route; ii) flawless operation in sweat or artificial sweat; and iii) distinguished sensing performance are the potentiometric electrodes listed in Table 1. However, potentiometric sensors inevitably require the use of a reference electrode—a limitation that they share also with ISFETs—which can be unfeasible for wearable technologies or can add complexity to the final application (for the case of devices employing integrated printed reference electrodes[55]). Here, our device operates based on voltage changes induced by the different cation concentrations that result in output current signals. The working range of our sensor (10^{-1} to 10^{-5} M) is wide enough to cover the typical K^+ and Na^+ concentrations found in sweat (namely from a few to hundreds millimolars) and its real-time response lies within the fastest reported sensors (Table 1). The reported rapid cation determination using ISM-functionalized plastic rGO LGTs can be a viable approach for sweat analysis aiming at health monitoring by employing devices truly compatible with wearable electronics technology.

4. Conclusion

In summary, we have reported on the fabrication of highly sensitive and selective sensors for the detection of cationic species in artificial sweat employing a potentially scalable and highly robust manufacturing process ready to be employed in future wearable health monitoring technologies. To achieve this goal, we combined the laser ablation of plastic Au-coated foils for the rapid prototyping of liquid-gated transistors (LGTs) with graphene oxide (GO) coating and its green in-situ electrochemical reduction (rGO) to produce the transducing units. The (aqueous) solution processability of GO endows large-area coatings at low costs that further contribute to the scalability of the device manufacturing method. Finally, analyte selectivity is achieved by functionalizing the rGO LGT channel with benchmark ion-selective membranes (ISMs) which allow the detection of K^+ and Na^+ in artificial sweat. The reported sensors showed excellent figures of merit, such as low working voltages (<0.5 V), fast (5–15 s) and linear response at a wide range of cation concentrations (from 10 μM to 100 mM), and sensitivities in the order of 1 μA/decade (K^+ or Na^+). Significantly, the employed laser-assisted patterning makes it possible to produce flexible electrodes with no need for photolithography, wet chemical methods (e.g., lift-off and etching) that typically employ hazardous chemicals, and an expensive cleanroom environment. In addition, the method allows the fabrication of microstructures featuring different shapes and configurations on nearly any surface, at high throughput, and most importantly, it is compatible with an industrial production line containing other manufacturing tools for plastic electronics. The robustness of this manufacturing process, as well as the technological relevance of our device, is fully demonstrated: similar products can be now purchased at Metrohm (https://www.dropsens.com/en/interdigitated_electrodes.html).

Supporting Information

Supporting Information is available from the Wiley Online Library or from the author.

Acknowledgements

The authors thank Ruslan R. A. Diduk and Arben Merkoçi from Institut Català de Nanociència i Nanotecnologia (ICN2) for fruitful discussions regarding paper fluidics, the VTT Technical Research Centre of Finland Ltd for furnishing paper membranes, and Marco Giannetto (Università di Parma) for fruitful discussions on the use of ISMs. The authors also acknowledge financial support from the EC through the ERC project SUPRA2DMAT (GA-833707), the Marie Sklodowska-Curie project ITN project BORGES (GA-813863), and the Graphene Flagship Core 3 project (GA-881603) as well as the Labex project CSC (ANR-10LABX-0026 CSC) within the Investissement d'Avenir program ANR-10-IDEX-0002-02 the International Center for Frontier Research in Chemistry and the Institut Universitaire de France (IUF). S.C. acknowledges the funding from the University of Padua, Department of Chemical Sciences (P-DiSC#11NexuS_BIRD2020-UNIPD-CARBON-FET-) and from the Italian Ministry of Education, Universities and Research (Nanochemistry for Energy and Health, NExuS, within the national funding network termed "Dipartimenti di Eccellenza"). R.F.O. acknowledges Gabrielle C. Lelis, Isabella Scarpa, and additional support from LNNano/Brazil (User Proposal AFM2-20220127).

Conflict of Interest

The authors declare no conflict of interest.

Data Availability Statement

The data that support the findings of this study are available from the corresponding author upon reasonable request.

Keywords

ion-selective membranes, laser ablation, liquid-gated transistors, reduced graphene oxide, wearable electronics

Received: March 24, 2022
Revised: May 22, 2022
Published online:

[1] K. S. Novoselov, A. Mishchenko, A. Carvalho, A. H. Castro Neto, *Science* **2016**, *353*, aac9439.
[2] M. Chhowalla, H. S. Shin, G. Eda, L.-J. Li, K. P. Loh, H. Zhang, *Nat. Chem.* **2013**, *5*, 263.
[3] S. Z. Butler, S. M. Hollen, L. Cao, Y. Cui, J. A. Gupta, H. R. Gutiérrez, T. F. Heinz, S. S. Hong, J. Huang, A. F. Ismach, E. Johnston-Halperin, M. Kuno, V. V. Plashnitsa, R. D. Robinson, R. S. Ruoff, S. Salahuddin, J. Shan, L. Shi, M. G. Spencer, M. Terrones, W. Windl, J. E. Goldberger, *ACS Nano* **2013**, *7*, 2898.
[4] R. Furlan de Oliveira, V. Montes-García, A. Ciesielski, P. Samorì, *Mater. Horiz.* **2021**, *8*, 2685.
[5] W. Zhang, Q. Wang, Y. Chen, Z. Wang, A. T. S. Wee, *2D Mater.* **2016**, *3*, 022001.
[6] S. Zhai, L. Wei, H. E. Karahan, X. Chen, C. Wang, X. Zhang, J. Chen, X. Wang, Y. Chen, *Energy Storage Mater.* **2019**, *19*, 102.
[7] C. Anichini, W. Czepa, D. Pakulski, A. Aliprandi, A. Ciesielski, P. Samorì, *Chem. Soc. Rev.* **2018**, *47*, 4860.
[8] O. C. Compton, S. T. Nguyen, *Small* **2010**, *6*, 711.
[9] D. Chen, H. Feng, J. Li, *Chem. Rev.* **2012**, *112*, 6027.
[10] S. Pei, H.-M. Cheng, *Carbon* **2012**, *50*, 3210.
[11] R. You, Y. Liu, Y. Hao, D. Han, Y. Zhang, Z. You, *Adv. Mater.* **2020**, *32*, 1901981.
[12] X. Huang, X. Qi, F. Boey, H. Zhang, *Chem. Soc. Rev.* **2012**, *41*, 666.
[13] R. K. Singh, R. Kumar, D. P. Singh, *RSC Adv.* **2016**, *6*, 64993.
[14] C. K. Chua, M. Pumera, *Chem. Soc. Rev.* **2014**, *43*, 291.
[15] Y. Sang, Z. Zhao, J. Tian, P. Hao, H. Jiang, H. Liu, J. P. Claverie, *Small* **2014**, *10*, 3775.
[16] W. Lv, D.-M. Tang, Y.-B. He, C.-H. You, Z.-Q. Shi, X.-C. Chen, C.-M. Chen, P.-X. Hou, C. Liu, Q.-H. Yang, *ACS Nano* **2009**, *3*, 3730.
[17] Y. Matsumoto, M. Koinuma, S. Y. Kim, Y. Watanabe, T. Taniguchi, K. Hatakeyama, H. Tateishi, S. Ida, *ACS Appl. Mater. Interfaces* **2010**, *2*, 3461.
[18] H. M. A. Hassan, V. Abdelsayed, A. E. R. S. Khder, K. M. AbouZeid, J. Terner, M. S. El-Shall, S. I. Al-Resayes, A. A. El-Azhary, *J. Mater. Chem.* **2009**, *19*, 3832.
[19] R. Furlan de Oliveira, P. A. Livio, V. Montes-García, S. Ippolito, M. Eredia, P. Fanjul-Bolado, M. B. González García, S. Casalini, P. Samorì, *Adv. Funct. Mater.* **2019**, *29*, 1905375.
[20] N. A. Kotov, I. Dékány, J. H. Fendler, *Adv. Mater.* **1996**, *8*, 637.
[21] G. K. Ramesha, S. Sampath, *J. Phys. Chem. C* **2009**, *113*, 7985.
[22] M. Pumera, A. Ambrosi, A. Bonanni, E. L. K. Chng, H. L. Poh, *TrAC, Trends Anal. Chem.* **2010**, *29*, 954.
[23] M. Bariya, H. Y. Y. Nyein, A. Javey, *Nat. Electron.* **2018**, *1*, 160.
[24] J. R. Sempionatto, I. Jeerapan, S. Krishnan, J. Wang, *Anal. Chem.* **2020**, *92*, 378.
[25] D. Paeng, J.-H. Yoo, J. Yeo, D. Lee, E. Kim, S. H. Ko, C. P. Grigoropoulos, *Adv. Mater.* **2015**, *27*, 2762.
[26] R. Qin, M. Hu, N. Zhang, Z. Guo, Z. Yan, J. Li, J. Liu, G. Shan, J. Yang, *Adv. Electron. Mater.* **2019**, *5*, 1900365.
[27] H.-L. Yeh, J. V. Garich, I. R. Akamine, J. M. Blain-Christen, S. A. Hara, in 2020 Des. Med. Devices Conf., American Society of Mechanical Engineers, Minneapolis, MN **2020**, p. V001T04A002.
[28] C. Strohhöfer, G. Klink, M. Feil, A. Drost, D. Bollmann, D. Hemmetzberger, K. Bock, *Meas. Control* **2007**, *40*, 80.
[29] I. Fakih, O. Durnan, F. Mahvash, I. Napal, A. Centeno, A. Zurutuza, V. Yargeau, T. Szkopek, *Nat. Commun.* **2020**, *11*, 3226.
[30] E. Zdrachek, E. Bakker, *Anal. Chem.* **2019**, *91*, 2.
[31] I. Fakih, A. Centeno, A. Zurutuza, B. Ghaddab, M. Siaj, T. Szkopek, *Sens. Actuators, B* **2019**, *291*, 89.
[32] H. Li, Y. Zhu, Md. S. Islam, M. A. Rahman, K. B. Walsh, G. Koley, *Sens. Actuators, B* **2017**, *253*, 759.
[33] K. Maehashi, Y. Sofue, S. Okamoto, Y. Ohno, K. Inoue, K. Matsumoto, *Sens. Actuators, B* **2013**, *187*, 45.
[34] T. A. Baldo, L. F. de Lima, L. F. Mendes, W. R. de Araujo, T. R. L. C. Paixão, W. K. T. Coltro, *ACS Appl. Electron. Mater.* **2021**, *3*, 68.
[35] L. Fusco, M. Garrido, C. Martín, S. Sosa, C. Ponti, A. Centeno, B. Alonso, A. Zurutuza, E. Vázquez, A. Tubaro, M. Prato, M. Pelin, *Nanoscale* **2020**, *12*, 610.
[36] M. Pelin, L. Fusco, V. León, C. Martín, A. Criado, S. Sosa, E. Vázquez, A. Tubaro, M. Prato, *Sci. Rep.* **2017**, *7*, 40572.
[37] N. Lago, M. Buonomo, R. C. Hensel, F. Sedona, M. Sambi, S. Casalini, A. Cester, *IEEE Trans. Electron Devices* **2022**, *69*, 3192.
[38] E. Bakker, A. J. Meir, *SIAM Rev.* **2003**, *45*, 327.
[39] H. Wang, Y. Wu, C. Cong, J. Shang, T. Yu, *ACS Nano* **2010**, *4*, 7221.
[40] N. Palavesam, W. Hell, A. Drost, C. Landesberger, C. Kutter, K. Bock, *Electronics* **2020**, *9*, 238.
[41] A. J. Bandodkar, W. J. Jeang, R. Ghaffari, J. A. Rogers, *Annu. Rev. Anal. Chem.* **2019**, *12*, 1.

[42] W. Dang, L. Manjakkal, W. T. Navaraj, L. Lorenzelli, V. Vinciguerra, R. Dahiya, *Biosens. Bioelectron.* **2018**, *107*, 192.
[43] M. Sarwar, P. Rodriguez, C. Li, *J. Anal. Test.* **2019**, *3*, 80.
[44] R. F. de Oliveira, S. Casalini, T. Cramer, F. Leonardi, M. Ferreira, V. Vinciguerra, V. Casuscelli, N. Alves, M. Murgia, L. Occhipinti, F. Biscarini, *Flexible Printed Electron.* **2016**, *1*, 025005.
[45] M. Tello, M. Chiesa, C. M. Duffy, H. Sirringhaus, *Adv. Funct. Mater.* **2008**, *18*, 3907.
[46] R. Negishi, M. Akabori, T. Ito, Y. Watanabe, Y. Kobayashi, *Sci. Rep.* **2016**, *6*, 28936.
[47] D. Park, J. H. Kim, H. J. Kim, D. Lee, D. S. Lee, D. S. Yoon, K. S. Hwang, *Biosens. Bioelectron.* **2020**, *167*, 112505.
[48] V. Pinkova Gajdosova, L. Lorencova, A. Blsakova, P. Kasak, T. Bertok, J. Tkac, *Curr. Opin. Electrochem.* **2021**, *28*, 100717.
[49] Q. Yuan, S. Wu, C. Ye, X. Liu, J. Gao, N. Cui, P. Guo, G. Lai, Q. Wei, M. Yang, W. Su, H. Li, N. Jiang, L. Fu, D. Dai, C.-T. Lin, K. W. A. Chee, *Sens. Actuators, B* **2019**, *285*, 333.
[50] P. Aspermair, V. Mishyn, J. Bintinger, H. Happy, K. Bagga, P. Subramanian, W. Knoll, R. Boukherroub, S. Szunerits, *Anal. Bioanal. Chem.* **2021**, *413*, 779.
[51] T. Han, U. Mattinen, J. Bobacka, *ACS Sens.* **2019**, *4*, 900.
[52] R. D. Shannon, *Acta Crystallogr., Sect. A: Found. Crystallogr.* **1976**, *32*, 751.
[53] T. Dudev, C. Lim, *J. Am. Chem. Soc.* **2010**, *132*, 2321.
[54] Z. Wang, J. Shin, J. Park, H. Lee, D. Kim, H. Liu, *Adv. Funct. Mater.* **2021**, *31*, 2008130.
[55] W. Gao, S. Emaminejad, H. Y. Y. Nyein, S. Challa, K. Chen, A. Peck, H. M. Fahad, H. Ota, H. Shiraki, D. Kiriya, D.-H. Lien, G. A. Brooks, R. W. Davis, A. Javey, *Nature* **2016**, *529*, 509.
[56] Q. An, S. Gan, J. Xu, Y. Bao, T. Wu, H. Kong, L. Zhong, Y. Ma, Z. Song, L. Niu, *Electrochem. Commun.* **2019**, *107*, 106553.
[57] C.-W. Lee, S.-Y. Jeong, Y.-W. Kwon, J.-U. Lee, S.-C. Cho, B.-S. Shin, *Sens. Actuators A Phys.* **2022**, *334*, 113320.
[58] H. Zhang, L. Sun, C. Song, Y. Liu, X. Xuan, F. Wang, J. Zhong, L. Sun, *Sens. Rev.* **2022**, *42*, 76.